

Finite temperature equations of state

Adriana R. Raduta
(adriana.raduta@nipne.ro)
IFIN-HH Bucharest, Romania

Collaborators: F. Nacu (IFIN-HH, Bucharest), M. Oertel (LUTH, Meudon, France)

For more, see arXiv: 2109.00251

The Modern Physics of Compact Stars and Relativistic Gravity,
September 27-30, 2021, Yerevan (Armenia) and virtually through Zoom

Finite temperature equations of state

Summary

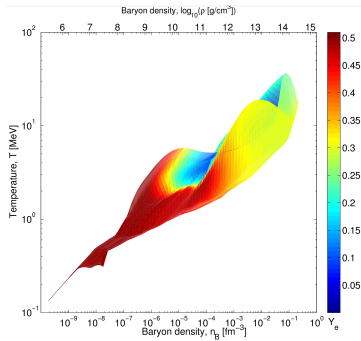
- Motivation
- Overview of presently available general-purpose EoSs on COMPOSE*
- Matter properties at finite temperatures: thermal energy density and pressure, heat capacities at constant volume and pressure, adiabatic and thermal index, speed of sound
- Correlations with the effective mass
- (The role of) effective mass in PNS and stellar BH formation: numerical simulations results
- Symmetry energy at finite- T
- Composition
- Testing Γ -law's reliability: proto-NS properties
- Conclusions

* <https://compose.obspm.fr/>

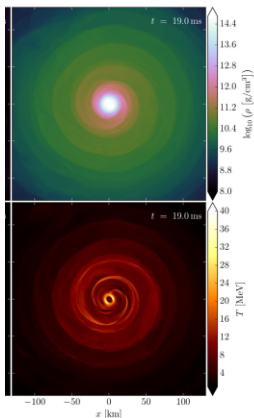
Complement to M. Oertel's talk on Monday

Finite-T EoSs - Why?

- in a series of astrophysical phenomena and environments – core-collapse supernovae, proto-NS, binary NS mergers, stellar BH – wide ranges of baryonic densities [$10^{-10} \leq n_B \leq 1 - 10 \text{ fm}^{-3}$], temperature [$0 \leq T \leq 100 \text{ MeV}$] and charge fraction [$0 \leq Y_q \leq 0.6$] are populated



Fischer et al., Eur. Phys. J A50 (2014)



CCSN [Fischer+, EPJA (2014)]

BNS: 19 ms post-merger [Endrizzi+, PRD 2018]

Finite-T EoSs (I): from 1991 to 2010 (two decades)

only two EoS models:

(1) Lattimer & Swesty (LS) [NPA 535, 331 (1991)]

(2) Shen, Toki, Oyamatsu & Sumiyoshi (STOS) [NPA 637, 435 (1998)]

Common features: inhomogeneous low density phase modeled within the Single Nucleus Approximation (SNA); in-medium surface modifications of cluster en. functional; only n, p, α ;

Specific features: non-relativistic (LS) vs. relativistic (STOS); the unique "heavy" nucleus is treated within liquid-drop approx. (LS) vs. extended Thomas Fermi (STOS); the transition inhomogeneous-homogeneous phases is done by Maxwell constr. (LS) versus minimization of free energy (STOS); different NM-param.

model	n_{sat} [fm ⁻³]	E_{sat} [MeV]	E_{sym} [MeV]	L_{sym} [MeV]	K_{sat} [MeV]	M_{max} [M_{\odot}]
LS180	0.155	-16.00	28.61	73.81	180	1.84
LS220	0.155	-16.00	28.61	73.81	219.85	2.06
LS375	0.155	-16.00	28.61	73.81	375	2.72
STOS	0.145	-16.26	36.89	110.79	281.16	2.23

Finite-T EoSs (II): since 2010

much more models...

- (3) Hempel & Schaffner-Bielich (HS) [NPA (2010)]: CDFT, extended NSE, various pools of nuclei in the low density phase
- (4) Shen, Horowitz, Teige & O'Connor [PRC (2011)]: CDFT, virial expansion
- (5) Schneider, Roberts & Ott (SRO) [PRC (2017)]: based on LS, allows for any Skyrme-like functional and APR ab-initio potential
- (6) Togashi et al. (TNTYST) [NPA (2017)]: based on STOS, Kanzawa et al. (KOST), NPA (2007) ab-initio
- (7) Raduta & Gulminelli (RG) [NPA (2019)]: Skyrme, extended NSE

More variability: non-relativistic/CDFT/ab-initio potentials; SNA and NSE; different modeling of the low density phase, including the transition to homogeneous matter; consideration of exotic particle d.o.f, especially for HS; broader coverage of NM param. space but not always in accord with constraints;

on August, 30: 91 models

Finite-T EoSs available on COMPOSE*

model	M_{max} (M_{\odot})	R_{14} (km)	$R_{2.072}$ (km)	$\bar{\Lambda}$ q=0.73	$\bar{\Lambda}$ q=1	exotica	L_{sym} [MeV]	K_{sat} [MeV]
LS220	2.06	12.7	-	664	596	Λ	73.81	219.85
SRO(APR)	2.16	11.3	10.9	299	272	no	58.47	266.0
SRO(NRAPR)	1.94	11.9	-	385	340	no	59.64	225.64
SRO(SLy4)	2.05	11.7	-	369	334	no	45.94	229.91
SRO(SkAPR)	1.97	12.0	-	535	490	no	58.47	266.0
SRO(LS220)	2.04	12.7	-	658	593	no	73.81	219.85
SRO(KDE0v1)	1.97	11.7	-	340	303	no	54.70	227.53
SRO(LNS)	1.72	11.0	-	235	196	no	33.43	210.76
STOS	2.23	14.5	13.7	1376	1279	$\Lambda; Y; Y\pi; q$	36.89	281.16
SNSH	2.12	13.1	12.5	793	756	no	31.38	281
TNTYST	2.21	11.5	11.1	358	332	no	35	245
DNS(CMF)	2.1	14.0	12.6	1114	1043	Yq	88	300
SHO	1.75	12.8	-	1182	932	no	60.44	229.54
SHO	2.12	13.6	14.2	2604	2307	no	60.50	229.54
SHT	2.78	14.9	14.9	1639	1555	no	118.53	271.53
FYSS	2.22	14.4	13.7	1376	1279	no	110.79	281.16
FT	2.25	11.5	11.1	360	334	no	35	245
HS(TM1)	2.21	14.5	13.7	1351	1255	no	110.79	281.16
HS(TMA)	2.02	13.8	-	1128	1052	no	90.14	318.15
HS(DD2)	2.42	13.1	13.1	799	758	$\Lambda; \Lambda\pi; Y; q$	55.04	242.72
HS(FSG)	1.74	12.6	-	539	439	no	60.44	229.54
HS(IUF)	1.95	12.7	-	608	570	no	47.21	231.33
SFHo	2.06	11.9	-	401	366	Y	47.10	245.4
SFHx	2.13	12.0	11.3	466	428	no	23.18	238.8
RG(SLy4)	2.07	11.9	-	369	334	no	45.94	229.91

* <https://compose.obspm.fr/> [Typel, Oertel & Klöhn (2015)]

$K_{sat} = 230 \pm 40$ MeV [Khan+, PRL (2012)]; $L_{sym} = 58.7 \pm 28.1$ MeV [Oertel+, RMP

Nuclear Matter EoS – a phenomenological perspective

Case study: Cold neutron matter $E(n_n, n_p)$

Phenomenological 2D Taylor around the minimum $(n_{sat}, 0)$,
power expansion as a function of $(n - n_{sat})$ and departure from isospin asymmetry

$$E/A(n, \delta) = E_{IS}(n) + \delta^2 E_{IV}(n) = e(n, \delta)/n, \quad \delta = (n_n - n_p)/(n_n + n_p)$$

$$\text{Isoscalar term: } E_{IS}(n) = E_{sat} + \frac{1}{2!} K_{sat} \chi^2 + \frac{1}{3!} Q_{sat} \chi^3 + \dots, \quad \chi = (n - n_{sat})/3n_{sat}$$

$$\text{Isovector term: } E_{IV}(n) = E_{sym} + L_{sym} \chi + \frac{1}{2!} K_{sym} \chi^2 + \frac{1}{3!} Q_{sym} \chi^3 + \dots$$

where E_{sat} , K_{sat} , E_{sym} , L_{sym} , K_{sym} , etc.

have physical meaning;

can be extracted from experiments;

are related to param. of the interaction;

see *Bao An Li's talk on Monday*

Nuclear Matter EoS – a microscopic perspective

Case study: Non-relativistic mean field models

E is the eigenvalue associated to \hat{H}

$$\text{en. density: } h(n, T) = \frac{\hbar^2}{2m} \tau + h_{\text{int}}(n, \tau),$$

$$\delta\langle\hat{H}\rangle = \int d\vec{r} \delta h = \text{Tr} \left(\left[\frac{\partial h}{\partial \tau} \frac{\hat{p}^2}{\hbar^2} + \frac{\partial h}{\partial n} \right] \delta \hat{n} \right),$$

$$\delta\langle\hat{H}\rangle = \text{Tr} \langle \hat{W} \delta \hat{n} \rangle$$

$$\text{effective mean-field } W = \frac{\partial h}{\partial \tau} \frac{\hat{p}^2}{\hbar^2} + \frac{\partial h}{\partial n} = \frac{\hat{p}^2}{2m^*} + U(n),$$

$$\text{single-part. en.: } \epsilon = p^2/2m^* + U(n),$$

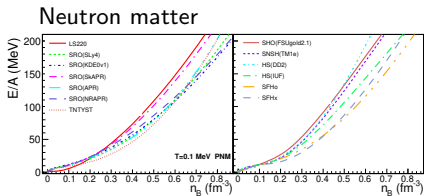
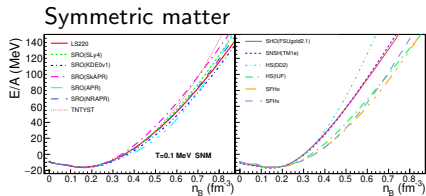
$$m^* = p \left[\left(\frac{d\epsilon}{dp} \right)_{p=p_F} \right]^{-1} \quad \text{Landau effective mass, 0-}T \text{ concept}$$

$$\text{for Skyrme: } m_i^* = \left[\frac{1}{m_i} + (C_{\text{eff}} n \pm D_{\text{eff}} n_3) \frac{2}{\hbar^2} \right]^{-1}$$

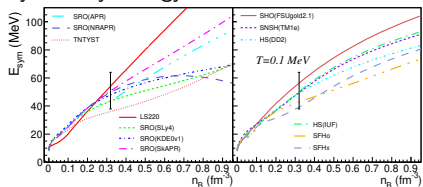
→ independent of momenta

[Vautherin, Adv. Nucl. Phys. 22 (1996)]

Properties of selected nucleonic models at $T = 0$



Symmetry energy



- 2 ab-initio models: APR and KOST
- 5 Skyrme-like models
- 6 CDFT models

Nuclear Matter EoS – at finite- T

en. density: $h(n, T) = \frac{\hbar^2}{2m} \tau + h_{int}(n, \tau)$,

effective mean-field $W = \frac{\partial h}{\partial \tau} \frac{\hat{p}^2}{\hbar^2} + \frac{\partial h}{\partial n} = \frac{\hat{p}^2}{2m^*} + U(n)$,

single-part. en.: $\epsilon = p^2/2m^* + U(n)$,

Where does T enter?

Distribution function: $f_{FD}(p) = [1 + \exp[\beta(\epsilon - \mu)]]^{-1}$,

where μ is such that $n = g \frac{4\pi}{h^3} \int_0^\infty f(p) p^2 dp$,
 $\tau = g \frac{4\pi}{h^3 \hbar^2} \int_0^\infty f(p) p^4 dp$,

m^* will impact finite- T behavior

simulations of early evol. of PNS, stellar BH formation confirms this

Covariant Density Functional Theory models

single-part. en.: $\epsilon = \sqrt{m_D^{*2} + p^2}$, $m_D^* = m - g_\sigma \sigma$, Dirac mass

Dirac versus Landau masses at $T=0$: $m_L^* = \sqrt{m_D^{*2} + p_F^2}$

Finite-T EoSs available on COMPOSE*

model	M_{max} (M_{\odot})	L_{sym} [MeV]	K_{sat} [MeV]	m_L^* (m_n)	Δm_L^* (m_n)
LS220	2.06	73.81	219.85	1.00	0.00
SRO(APR)	2.16	58.47	266.0	0.698	0.211
SRO(NRAPR)	1.94	59.64	225.64	0.694	0.214
SRO(SLy4)	2.05	45.94	229.91	0.695	-0.184
SRO(SkAPR)	1.97	58.47	266.0	0.694	0.214
SRO(LS220)	2.04	73.81	219.85	0.694	0.214
SRO(KDE0v1)	1.97	54.70	227.53	0.744	-0.128
SRO(LNS)	1.72	33.43	210.76	0.826	0.228
STOS	2.23	36.89	281.16	0.689	0.085
SNSH	2.12	31.38	281	0.647	0.086
TNTYST	2.21	35	245	n.a	n.a.
DNS(CMF)	2.1	88	300	n.a	n.a.
SHO	1.75	60.44	229.54	0.668	0.089
SHO	2.12	60.50	229.54	0.668	0.089
SHT	2.78	118.53	271.53	0.659	0.090
FYSS	2.22	110.79	281.16	0.689	0.085
FT	2.25	35	245	n.a	n.a.
HS(TM1)	2.21	110.79	281.16	0.689	0.085
HS(TMA)	2.02	90.14	318.15	0.686	0.086
HS(DD2)	2.42	55.04	242.72	0.626	0.097
HS(FSG)	1.74	60.44	229.54	0.668	0.089
HS(IUF)	1.95	47.21	231.33	0.670	0.093
SFHo	2.06	47.10	245.4	0.811	0.078
SFHx	2.13	23.18	238.8	0.771	0.083
RG(SLy4)	2.07	45.94	229.91	0.695	-0.184

m_L^* Landau eff. mass in
SNM at n_{sat}

Δm_L^* mass splitting in PNM
at at n_{sat}

Δm_L^* depends on m_S^* , m_V^* ;
 m_V^* dep. on sym. en.

CDFT: $\Delta m_L^* > 0$

Skyrme: $\Delta m_L^* > 0$, $\Delta m_L^* < 0$

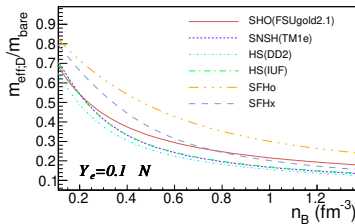
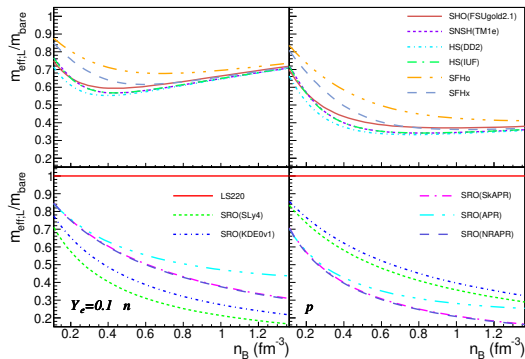
microscopic with 3N:
 $\Delta m_L^* > 0$

[B.A. Li+, Prog. Part. Nucl.
Phys. (2018)]

* <https://compose.obspm.fr/> [Typel, Oertel & Klöhn (2015)]

Properties of selected nucleonic models at $T = 0$

Effective masses as a function of density



Landau eff. masses

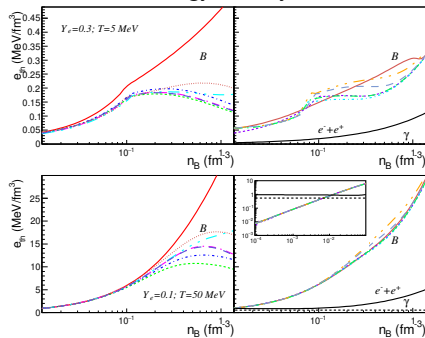
- m_L^* qualitatively different in CDFT, Skyrme & APR models
- m_L^* more scattered in Skyrme
- $m^*(NRAPR) \neq m^*(APR)$, corr. in APR cannot be accounted for by Skyrme-like int.

Dirac eff. masses

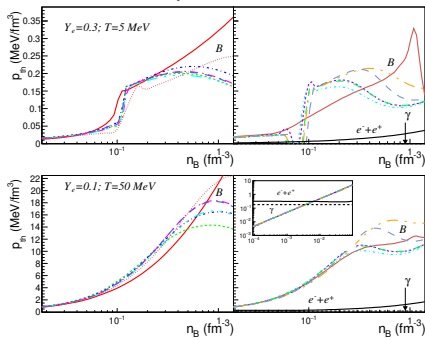
Thermal effects

$$X_{th} = X(n_B, Y_e, T) - X(n_B, Y_e, 0)$$

energy density



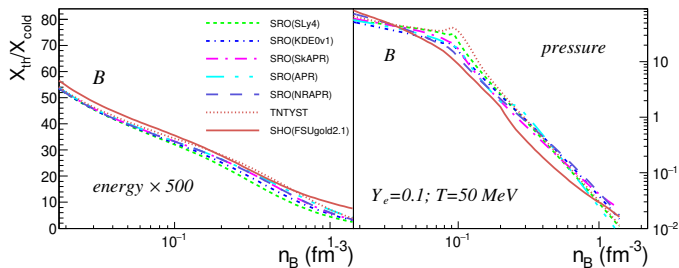
pressure



- at low n_B , ideal gas behavior
- at high n_B , EoS-dep.
- over $0.1 \lesssim n_B \lesssim 0.2 - 0.5 \text{ fm}^{-3}$ correl. e_{th} , p_{th} and m^* [Constantinou et al., PRC (2014)]

- at high n_B , a diversity of behaviors
 - ▶ LS220: ideal gas
 - ▶ qualitative difference among Skyrme and CDFT
- electron & photon contrib.

Thermal effects – significance as a function of density



- the higher the density, the smaller the thermal effects
- modifications induced on the pressure (energy) are (not) important
- strong EoS-dependence of p_{th}

Γ -law , Γ_{th}

Context: until recently a small number of finite- T EoS were available

Solution: phenomenological extension of cold EoS

① **Γ -law:** $P(n_B, e) = P_{cold}(n_B) + (\Gamma - 1) e_{th}(n_B),$

- ▶ Γ constant, typically $1.5 \leq \Gamma \leq 2$
- ▶ no T , n_B , composition-dependence

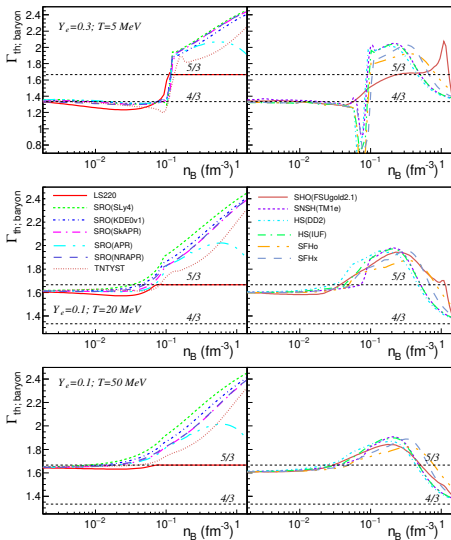
[Bauswein+ (2010); Hotokezaka+ (2013); Endrizzi+ (2018); Camelio+ (2019)]

② $\Gamma = 1 + p_{th}/e_{th} = \Gamma_{th},$

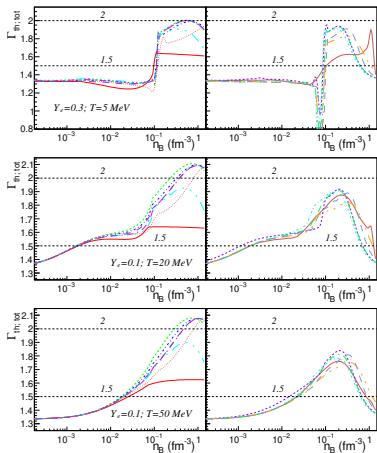
- ▶ test of Γ -law, see next

③ M^* -approximation [Raithel+, (2019)]: parameterized $p_{th}(n_B, Y_p, T)$; params. dependent on E_{sym} and $m^*(n_B)$; probably different laws for CDFT/Skyrme/ab initio

Γ_{th} : baryon contribution



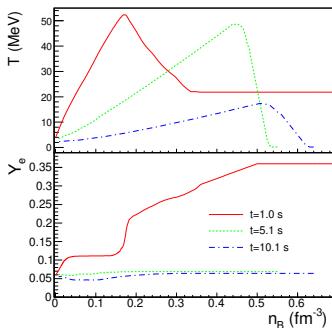
- strong n_B and EoS dep.;
at low T , also T dep.
- low n_B : common behavior; no-EoS dep.;
 $\lim_{n_B \rightarrow 0; \text{high } T} = 5/3$, classical limit for dilute gas
- high n_B : strong EoS-dep.; for CDFT
 $\Gamma_{th} \rightarrow 4/3$, ultra-rel. gases
- CDFT models show a maximum; corr.
with a minimum in m^*
- $\Gamma_{th}(LS) \neq 5/3$ because of clusters
- see [Constantinou+, PRC (2015)]

Γ_{th} 

- electrons and photons induce only quantitative changes;
- at low n_B , $\Gamma_{th} < 1.5$
- at high n_B and high T , Skyrme and TNTYST give $\Gamma_{th} > 2$
- at high n_B , CDFT give $\Gamma_{th} < 1.5$
- for $T > T_C$, weak T -dep.
- weak Y_p -dep.
- Γ -law is a crude approx.

Γ_{th} reliability test

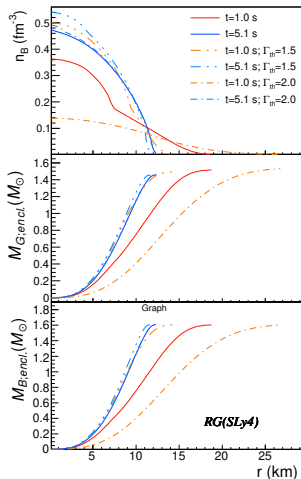
Case study: properties of PNS



evolution of PNS

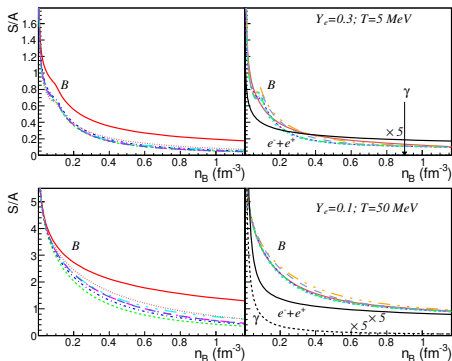
$M_B = 1.6M_{\odot}$; RG(SLy4) EoS

[Pascal, PhD thesis, LUTH-Meudon, 2021]



- as long as $n_B \lesssim n_{sat}$ are hot, Γ -low does not provide a good estimation

Entropy



- large EoS-dep.
- large m^* provide large S/A
- role of electrons and photons
- specific heats at const. volume and pressure

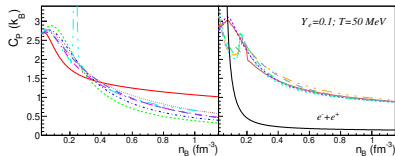
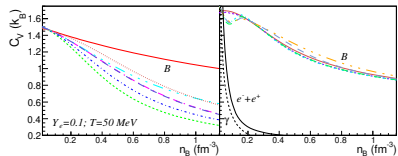
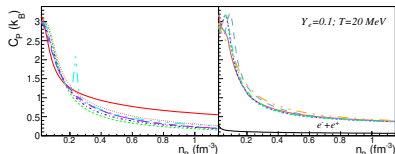
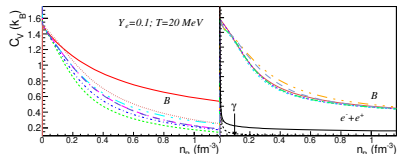
$$C_V = T \left(\frac{\partial(S/A)}{\partial T} \right) \Big|_{V, \{N_i\}}$$

$$C_V \text{ will replicate the behavior of } S/A, \text{ including corr. with } m^*$$

$$C_P = T \left(\frac{\partial(S/A)}{\partial T} \right) \Big|_{P, \{N_i\}}$$

$$= C_V + T/n_B^2 \left(\frac{\partial P}{\partial T} \Big|_n \right)^2 / \left(\frac{\partial P}{\partial n} \right) \Big|_T$$
 complex behavior as P dep. on m^* , dm^*/dn_B

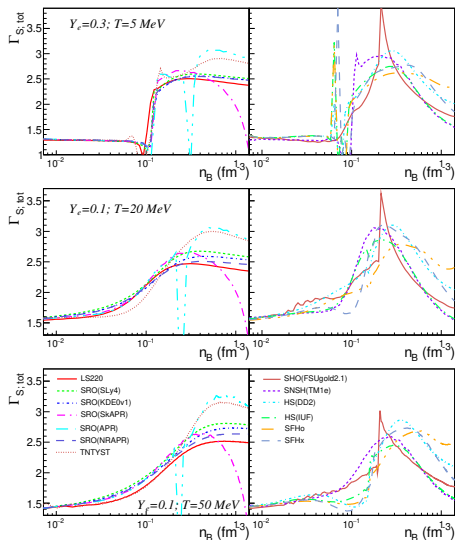
Specific heat capacities



- similar behavior for all models
- $\lim_{n_B \rightarrow 0} C_V = 3/2$, as Boltzmann gases
- C_V decreases with n_B
- large m^* , large C_V
- electrons, photons

- similar behavior for all models
- APR: discontinuity due to π condensate
- $\lim_{n_B \rightarrow 0} C_P$ is T -dep.
- high- T : $\lim_{n_B \rightarrow 0} C_P = 5/2$, Boltzmann gases
- C_P has a maximum at low- n_B ; for the non-degenerate limit, see [Constantinou+(2014)]; C_P decreases with n_B
- more complex EoS-dep. behavior than C_V

Adiabatic index

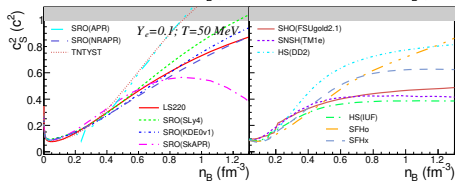
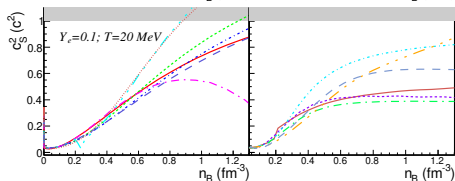
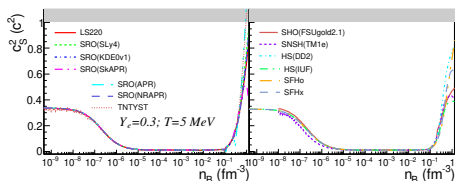


baryons+electrons+photons

$$\Gamma_S = \left. \frac{\partial \ln P}{\partial \ln n_B} \right|_S = \frac{C_P}{C_V} \frac{n_B}{P} \left. \frac{\partial P}{\partial n_B} \right|_T$$

- EoS stiffness in const.- S processes
- similar behavior but EoS-dep.
- strong (weak) on n_B (T and Y_p)
- APR: discontinuity due to π condensate
- no obvious effect of m^*
- at low T and $n_B < n_t$, $\Gamma_S \neq 0$ as LG phase coexistence is suppressed by the electron gas

Speed of sound



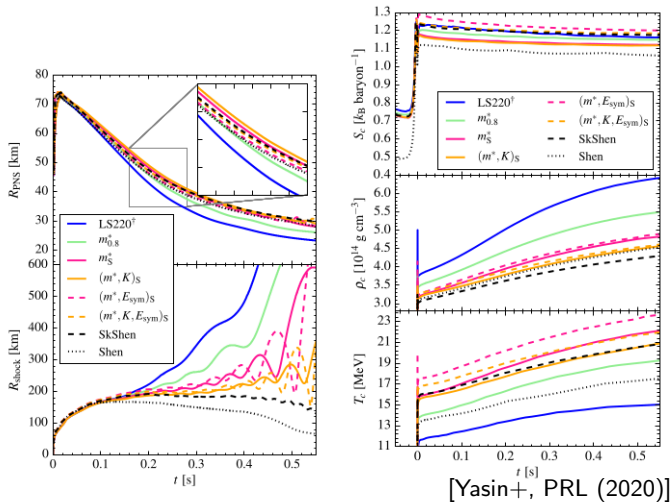
baryons+electrons+photons

$$\frac{c_s^2}{c^2} = \left. \frac{dP}{de} \right|_{S,A,Y_e} = \Gamma_S \frac{P}{e + P}$$

- $c_s/c > 1$ in non-relativistic models
- non-monotonic dep. on n_B for SkAPR
- strong dep. on n_B
- dissimilar behavior at low versus high T
- APR: discontinuity due to π condensate
- no obvious effect of m^*
- the low- n_B increase of c_s is due to the electron gas

m^* -effect in early post-bounce evolution

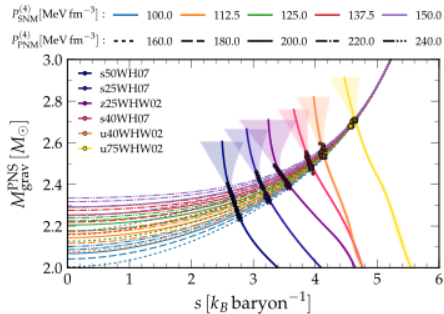
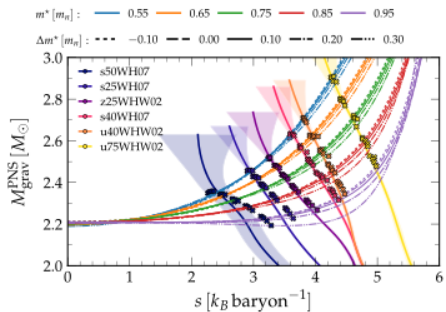
$m^*/m = 1$ (LS220), 0.634 (Shen)



large $m^* \rightarrow$ fast explosion; fast contraction of PNS; high (low) ρ_c (T)

large $m^* \rightarrow$ high (low) T (n_B and R) in the ν -sphere; large E_ν , L_ν [Schneider+, ApJ(2020)]

m^* -effect in the onset of collapse

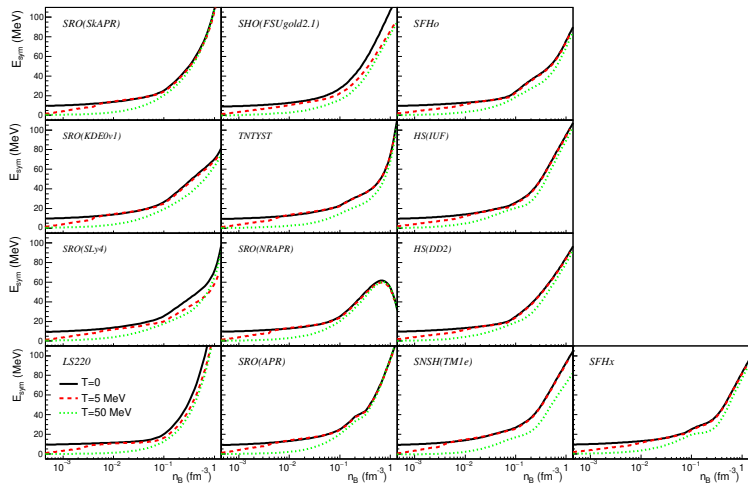


[Schneider et al., ApJ (2020)]

failed CCSN; stellar BH formation;

simulation results: collapse begins when hot core's gravitational mass exceeds the maximum gravitational mass predicted by the EoS under the specific thermo conditions;
 most important ingredients: progenitor and m^*

Symmetry energy, $E_{\text{sym}} = E_{\text{SM}} - E_{\text{PM}}$, at finite- T

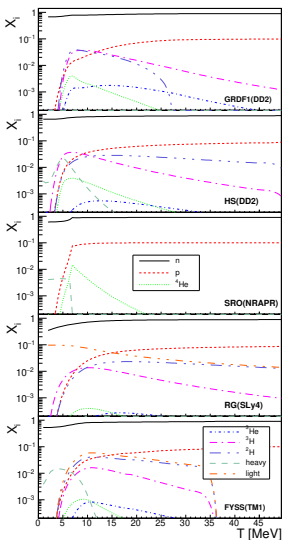


- at low- T $\lim_{n_B \rightarrow 0} \neq 0$; dis-homogeneity effect
- at high- T $\lim_{n_B \rightarrow 0} \rightarrow 0$, as in homogeneous matter
- T -dep. is non-monotonic, e.g. SRO(SLy4)
- $E_{\text{sym}}(T)$ in homo. matter [Ou+, PLB (2011)]

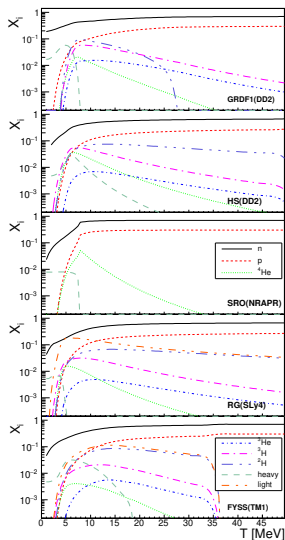
Composition as a function of T

$$n_B = 10^{-2} \text{ fm}^{-3}$$

$$Y_p = 0.1$$



$$Y_p = 0.3$$



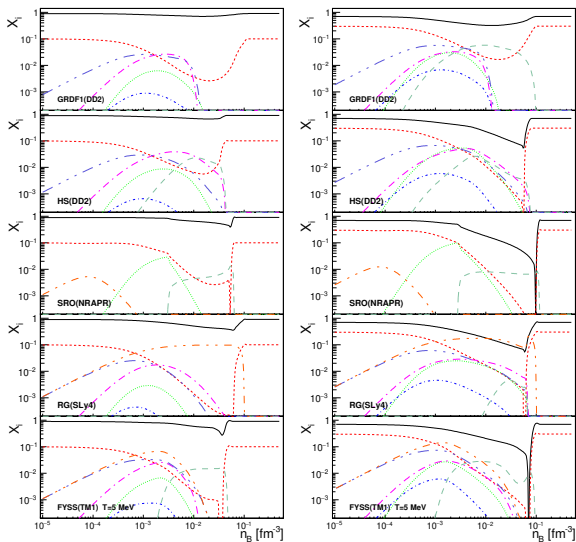
- SNA [SRO(NRAPR)] versus NSE [all other]
- SRO(NRAPR) and FYSS(TM1): the "heavy" clusters disappear at $T \approx T_C$;
- "light" clusters survive at $T > T_C$; abundances increases with T ;
- more clusters in sym. matter
- model-eff. important when nuclei are abundant

Composition as a function of n_B

$T = 5 \text{ MeV}$

$Y_p = 0.1$

$Y_p = 0.3$



- at low n_B , unbound nucleons dominate

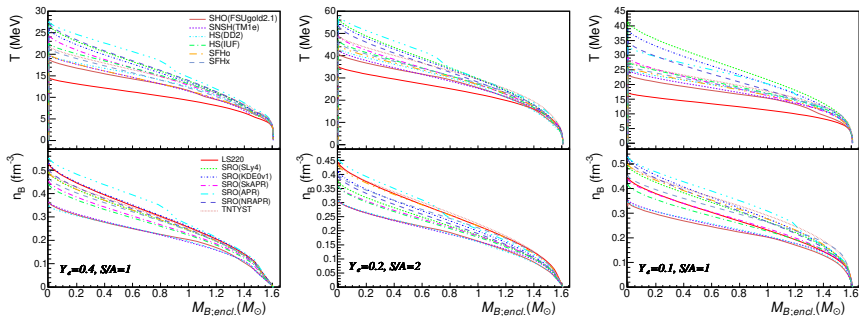
- model-dep. over $n_t(T)/100n_B \lesssim n_t(T)$

- for GRDF cluster dissolution at $n_B \approx n_t/10$

- excluded volume effects \rightarrow sudden transition to homo. matter

- more clusters in sym. matter

Properties of hot compact stars and the role of EoS



- strong EoS-dependence
- T -profiles reflect $m^*(n_B)$ [T (LS220) is the lowest; HS(DD2), SNSH(TM1e), SHO(FSUgold2.1) provide similar n_B -profiles and, thus, similar T -profiles; for $S/A = 1$, $Y_e = 0.1$ T (SLy4) $>$ T (NRAPR) $>$ T (SFHo)]
- for given S/A , large Y_p lead to low T
- π -condens. in APR produces a bump in radial profiles
- high S/A config. are more dilute

Conclusions

- Thermal effects are dominated by the density-dep. of the nucleons' effective mass, which is not constrained by nuclear physics experiments
- Γ -law does is not accurate enough
- Presently available realistic EoS do not exhaust the parameter space
- Role of exotic particle d.o.f. not yet investigated
- PNS properties strongly depend on EoS
- Numerical simulations show an important role of m^*